Dual-Layer PBI/P84 Hollow Fibers for Pervaporation Dehydration of Acetone

Gui Min Shi, Yan Wang, and Tai-Shung Chung
Dept. of Chemical and Biomolecular Engineering, National University of Singapore, 4 Engineering Drive 4, Singapore 117576

DOI 10.1002/aic.12625
Published online April 27, 2011 in Wiley Online Library (wileyonlinelibrary.com).

Acetone dehydration via pervaporation is challenging, because acetone and water have close molecular sizes, and acetone has a much higher vapor pressure than water. Acetone is also a powerful solvent, which dissolves or swells most polymers. We have developed novel polybenzimidazole/BTDA-TDI/MDI (PBI/P84) dual-layer hollow fibers for pervaporation dehydration of acetone for industrial and biofuel separations. Both thermal and chemical crosslinking modifications were applied to the membranes to investigate their effectiveness to overcome acetone-induced swelling. Thermal treatment can effectively enhance separation performance, but performance stability can only be achieved through the crosslinking modification of PBI. Crosslinking by p-*xylene dichloride followed by a thermal treatment above 250°C show significant effectiveness to improve and stabilize pervaporation performance. The fractional free volume of the PBI selective layer reduces from 3.27 to 1.98% and 1.33%, respectively, after thermal treatment and a combination of chemical/thermal crosslinking modifications characterized by positron annihilation spectroscopy.* © 2011 American Institute of Chemical Engineers *AIChE J,* 58: 1133–1145, 2012

Keywords: pervaporation dehydration, polybenzimidazole, dual-layer hollow fiber membrane, acetone, thermal treatment, crosslinking

Introduction

Acetone is a widely used solvent and an important raw material for the production of methyl methacrylate and bisphenol-A. It is mainly derived from the oxidation of cumene or propene.[1,2] It can also be produced from fermentation routes such as acetone-butanol-ethanol process.[1] Dewatering is a critical issue during acetone purification and production. Although acetone does not form azeotrope with water, its dehydration by conventional separation processes such as distillation is still energy intensive, because the two components have almost the same volatility when acetone concentration is 96 mol %.[3]

Correspondence concerning this article should be addressed to T.-S. Chung at chencts@nus.edu.sg.

© 2011 American Institute of Chemical Engineers

Pervaporation is a promising technology for molecular-scale liquid/liquid separations existing in biorefinery, petrochemical, and pharmaceutical industries because of its highly selective, economical, energy-efficient, and eco-friendly characteristics.[4–8] As only part of the feed is vaporized and the remaining feed does not undergo phase change, the pervaporation process consumes much less energy than the conventional distillation process. Pervaporation has gradually gained acceptance in industries to overcome the quality and energy problems in organic dehydration in recent years.

Table 1 shows the basic physicochemical properties of water and acetone. The pervaporation dehydration of acetone is challenging not only because acetone has a much higher vapor pressure (i.e., higher driving force) and close molecular size[9] compared to water, but also acetone is a powerful solvent aggressive to swell up polymeric materials. The former lowers the separation factor, whereas the later

Table 1. Basic Properties of PBI, P84, Water, and Acetone

Properties	PBI	P84	Water	Acetone
Kinetic diameter (nm)[9]	–	–	0.296	0.469
Vapour pressure (20°C)(kPa)*	–	–	2.31	24.6
Boiling point (°C)*	–	–	100	56.5
Viscosity (20°C)(mPa s)*	–	–	1.00	0.294
Solubility parameter $(MPa)^{1/2}$	33.7[10]	26.9[11]	47.9[11]	20.0[11]
Density (kg/m^3)	1.31[12]	1.30[11]	1.00	0.79

*Properties obtained from AspenTech DISTIL 2004.1.

deteriorates long-term separation performance. Several approaches have been proposed to reduce the polymeric swelling in pervaporation including thermal treatment,[13] crosslinking,[14-16] and blending with a more antiswelling polymer.[17,18]

Till date, only a few polymer materials have been reported on the pervaporation dehydration of acetone. Pioneer studies on membranes for acetone dehydration used highly hydrophilic polymeric membranes such as alginate,[19] chitosan,[20] and PVA[21] with the aid of various modifications because the original materials are not suitable for harsh feed environments. To enhance chemical resistance, Ray and Ray[22,23] studied PAN-maleic anhydride copolymer and poly(acrylonitrile-*co*-hydroxyethyl methacrylate) for acetone dehydration. Zhao et al.[24] investigated block copolymer membranes made of PAN-*b*-poly(ethylene glycol)-*b*-PAN with various types of poly(ethylene glycol). Amnuaypanich and Ratpolsan[25] examined the swelling problem of natural rubber latex grafted with poly(2-hydroxyethyl methacrylate) in water-acetone mixtures without proposing effective ways to suppress it. Commercial membranes, polyelectrolyte composite membrane (Symplex, GKSS), studied by Urtiaga et al.,[26] showed a high flux but a low-separation factor for the dehydration of acetone. So far, no much data on long-term separation performance have been reported. Therefore, the objectives of this work are to (1) investigate the science and engineering of designing suitable polymeric membranes for acetone dehydration in harsh environments, (2) study their performance stability before and after various chemical modifications, and (3) examine morphological and molecular-level changes by means of advanced instruments including positron annihilation spectroscopy (PALS).

Previous studies on acetone dehydration mainly emphasized on flat membranes. Hollow fiber configuration was chosen in this project, because it has been widely used in gas separation and other membrane processes, and it offers unique advantages of large surface to volume ratio, mechanical self-support, and high-packing density. Polybenzimidazole (PBI) is our focused material in this study, because it has excellent chemical resistance and thermal stability. PBI is a class of heterocyclic amorphous polymer, and the commercially available PBI has a chemical structure of poly-2,2′-(*m*-phenylene)-5,5′-bibenzoimidazole with a high T_g of 425–435°C. This material is a highly hydrophilic amorphous polymer with a reported water sorption up to 15–18 wt %.[27] Owing to these excellent properties, it has been studied for applications such as nanofiltration,[28] gas separation,[29] and fuel cell.[30] However, despite so many advantages, the application of PBI material as pervaporation membranes is very limited.[10,31] This is possibly due to the fact that the nonsolvent-induced phase-inversion PBI membrane is very brittle after drying.

To overcome the constrain, this article reports a novel coextruded dual-layer hollow fiber membrane consisting of a PBI functional separation layer and a P84 supporting layer with various post-treatment modifications for the pervaporation dehydration of acetone. To our best knowledge, the first pervaporation study using dual-layer hollow fibers was made of P84/ polyethersulfone (PES) for IPA dehydration.[32] Since then, many progresses have been made.[31–35] It is found that synergistic separation performance may be achievable for organic dehydration if inner- and outer-layer materials are properly selected even without much post-treatment. In this work, BTDA-TDI/MDI (P84) is used as the supporting layer material because of its relatively high hydrophobicity, good chemical resistance and mechanical strength, and less water-induced swelling.[36] The fundamental science and engineering of fabricating PBI/P84 hollows fibers with desirable membrane morphology and separation performance will be revealed. In addition, the effects of thermal and chemical crosslinking modifications on swelling characteristics, performance enhancement, and stability of separation performance will be systematically studied.

Experimental

Materials

The PBI polymer solution was purchased from Hoechst Celanese, with a composition of PBI (25.6 wt %), *N*-dimethylacetimide (DMAc; 72.4 wt %), and LiCl (2.0 wt %). The P84 (BTDA-TDI/MDI), copolyimide of 3,3′,4,4′-benzophenone tetracarboxylic dianhydride (BTDA) and 80% toluene diisocyanate (TDI) + 20% methylene diphenyl diisocyanate (MDI), was purchased from HP Polymer, Austria. P84 was dried in an oven at 120°C under vacuum overnight before use. Figure 1 shows PBI and P84 chemical structures. DMAc, *N*-methylpirolydone (NMP), *p*-xylene dichloride, methanol, and acetone were purchased from Sigma Aldrich and were used as received.

Spinning process and modules fabrication

Detailed description of single-layer and dual-layer hollow fiber spinning systems can be referred elsewhere,[32] and Table 2 lists the detailed spinning conditions for the single- and dual-layer coextrusion processes. The polymer solutions were degassed for 24 h before loading into a syringe pump (ISCO 1000), followed by overnight degassing again. A mixture of 90/10 (wt/wt %) NMP/water was used as the bore fluid to make a porous inner surface to minimize the substructure resistance. Both dope and bore fluids were filtered through 15-μm sintered metal filters before entering the dual-layer spinneret. Polymer solutions and bore fluid were extruded by three ISCO syringe pumps through a spinneret at room-temperature with an air gap of 2.5 cm and then immersed in a water coagulation bath. The as-spun hollow fibers were stored in tapping water for 3 days to remove residual solvents with fresh water daily.

The as-spun hollow fiber membranes were solvent-exchanged by methanol and followed by hexane. Each solvent exchange repeated three times and each time was for 30 min, and then the hollow fibers were dried in air naturally. The pervaporation module was prepared by loading

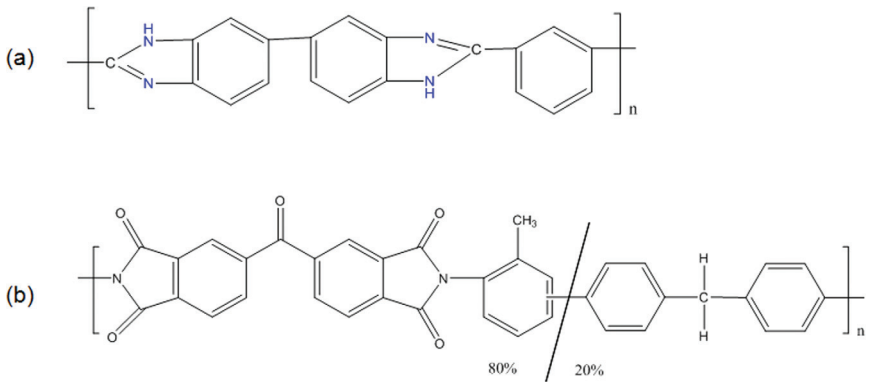

Figure 1. Chemical structures of (a) PBI and (b) P84-*co*-polyimide.

[Color figure can be viewed in the online issue, which is available at wileyonlinelibrary.com.]

one or two pieces of hollow fibers membranes into a polypropylene module with an effective length of around 15 cm. Both ends were sealed by epoxy and cured for at least 24 h at ambient temperature. Thermal treatment and chemical modification were carried out on individual hollow fibers before module fabrication.

Thermal treatment and chemical crosslinking modifications of PBI/P84 dual-layer fibers

The thermal treatment of hollow fibers was carried out in a vacuum oven with a temperature increment rate of 0.6°C/min from room-temperature to the desired temperature, held there for two hours, and then cooled it down naturally. The chemical crosslinking modification was conducted by immersing the hollow fiber membranes in a *p*-xylene dichloride/methanol solution at 40°C under agitation for the stipulated durations, followed by washing with fresh methanol. The hollow fibers were then dried in air naturally overnight or under further thermal treatment. Table 3 summarizes the post-treatment conditions of the membranes.

Sorption tests

The PBI and P84 dense films were fabricated by using a 15 wt % polymer solution in DMAc. The detailed preparation procedures was described elsewhere.[37] The strips of the dense films were dried under vacuum at 120°C overnight to remove absorbed moisture. Then these preweighed dry membrane strips were immersed in deionized water and pure acetone solutions at room-temperature, respectively. The swollen samples were taken out at different time intervals, blotted between tissue papers, and then weighed in a closed container. The degree of swelling was calculated from the difference between the wet weight M_{wet} at the sorption equilibrium and the dry weight M_{dry} as follows:

$$\text{Sorption } (\text{g/g membrane}) = \frac{M_{\text{wet}} - M_{\text{dry}}}{M_{\text{dry}}} \tag{1}$$

Pervaporation experiments

A laboratory scale pervaporation unit was used, and the details of the set up have been described elsewhere.[33] A feed solution of acetone/water (85/15 wt %) was used. The feed flow rate was maintained at 20 L/h for each module. The feed temperature was maintained at 50 ± 1°C unless otherwise specified. The permeate pressure was maintained less than 2 mbar by a vacuum pump. Retentate and permeate samples were collected after the membrane being conditioned for at least 2 h. The flux, J, was determined by the mass of permeate divided by the product of the interval time and membrane area. The mass of permeate was weighed using a Mettler Toledo balance. The separation factor, α, is defined by the equation below:

$$\alpha_{1/2} = \frac{y_{w1}/y_{w2}}{x_{w1}/x_{w2}} \tag{2}$$

where subscripts 1 and 2 refer to water and acetone, respectively. y_w and x_w are the weight fractions of a component in the permeate and feed and were analyzed using a Hewlett-Packard GC 7890 with a HP-INNOWAX column (packed with crosslinked polyethylene glycol) and a TCD detector.

Table 2. Spinning Conditions of Hollow Fiber Membranes

Spinning Conditions	PBI/P84 Dual-Layer	PBI single-Layer	PBI/P84 singal-Layer
Outer dope solution (wt %)	PBI/DMAc/LiCI	PBI/DMAc/LiCI	P84/DMAc
Outer dope flow rate (mL/min)	0.4	0.6	1.0
Inner dope solution	P84/DMAc (25/75)	–	–
Inner dope flow rate (mL/min)	1.0	–	–
Bore fluid flow rate (mL/min)	0.6	0.4	0.5
Take up speed (m/min)	4	2.7 (free fall)	5.1 (free fall)
Bore fluid composition (wt %)		NMP/Water(90/10)	
Air gap (cm)	2.5		
External coagulant		Tap water (Room temperature)	

Table 3. List of Post-treatment Conditions of Membranes

Membrane ID	*p*-Xylene Dichloride/Methanol	Thermal Treatment Temperature (°C)
X2*	2%	–
X2-T150*	2%	150
X2-T250*	2%	250
X2-T350*	2%	300
T-250	–	250
T-350	–	300
T-400	–	400
T-450	–	450

*Membranes are cross-linked for 2 h.

The flux and separation factors were converted to permeance and selectivity by the following approach. The partial vapor pressure of component i at the feed side was calculated according to the following equation with the aid of the AspenTech DISTIL 2004.1[38]:

$$f_i = x_i \gamma_i P_{i'}^{sat} \tag{3}$$

where x_i is the mole fraction of component i in the feed, and γ_i is the activity coefficient calculated by the Wilson equation. The saturated vapor pressure $P_{i'}^{sat}$ is determined by the Antoine equation. Both γ_i and $P_{i'}^{sat}$ were calculated with AspenTech DISTIL 2004.1. Based on the solution–diffusion mechanism, the basic transport equation for pervaporation can be expressed as

$$J_i = \frac{P_i}{l}(x_i \gamma_i P_{i'}^{sat} - y_i P^p) \tag{4}$$

where P_i is the membrane permeability of component i and is a product of diffusivity and solubility coefficient, l is the membrane thickness, y_i is the permeate mole fraction of component i, and p^p is the total pressure at the permeate side. The term P_i/l is known as the permeance of component i that can be determined if other terms are known. Permeability and permeance take into account of vapor pressure difference across membrane and eliminate the influence of operating conditions on membranes; hence comparisons of membranes under different operating conditions become possible. The membrane selectivity $\beta_{i,j}$ is defined as the permeability ratio or permeance ratio of components i to j.

Characterizations

PALS Characterization The PALS experiments were carried out using a variable monoenergy beam (0–30 keV). An HP Ge detector (EG&G Ortec. with 35% efficiency and energy resolution of 1.5 keV at 511 keV peak) was used to measure the Doppler broadening energy spectra (DBES) with a counting rate of approximately 3400 cps. The S parameter, defined as a ratio of integrated counts between 510.3 and 511.7 keV, to total counts after subtracting the background noise counts, measures the relative value of the low-momentum part of positron electron annihilation. The S parameters of DBES were measured as a function of positron incident energy (mean depth) at ambient temperature. The total number of counts for each DBES was 1.0 million. The PALS was coupled with the slow positron beam to study positron annihilation lifetime of membrane samples. The resolution of positron annihilation lifetime was 450–800 ps for a counting rate of 100–500 cps with each lifetime spectrum contains one million counts. Ortho-Positronium (O-Ps) was formed when positron and electrons in polymeric local free volume holes annihilates and had a lifetime range between 2–4 ns. The o-Ps lifetime, t_3, was obtained by fitting PALS spectroscopy data into three lifetime components using the PATFIT program.[39,40]

Other Characterizations The membrane morphology was observed by using a JSM-6700F field emission scanning electron microscope (FESEM). Samples were prepared by fracturing membranes in liquid nitrogen then coated with platinum. Wide-angle X-ray diffraction (XRD) measurements of the membranes were carried out by a Bruker X-ray diffractometer (Bruker D8 advanced diffractometer) at ambient temperature using the CuKα radiation wavelength ($\lambda = 1.54$ Å) at 40 kV and 30 mA. An X-ray photoelectron spectrometer (Kratos XPS System-AXIS His-165 Ultra) was used to measure the surface chemical compositions of the original and crosslinked PBI/P84 dual-layer hollow fibers. attenuated total reflectance-Fourier transform infrared spectroscopy (ATR-FTIR) analyses were performed using a Perkin–Elmer FTIR Spectrum 2000 with a resolution of 2 cm^{-1}. The spectra were obtained with an average of 16 scans.

Results and Discussion

Sorption tests of PBI and P84 dense films

Swelling by permeants on polymeric pervaporation membranes has a great effect on membrane performance and stability. As the membrane contacts the liquid feed side directly, the feed components will interact with the membrane through various intermolecular interactions. The higher affinity of the permeant to the polymeric membrane, the more predominant plasticizer the permeant is to the membrane.[11] If the solvent such as acetone is the predominant plasticizer, more severe swelling may be resulted from its larger kinetic size than water, leading to a much loosen polymer matrix and declined separation performance.

To investigate the inherent affinities of PBI molecules with permeating components, sorption tests of PBI dense membranes in acetone and water are carried out. The P84 material, used as the inner-layer of the dual-layer hollow fiber membranes, is also investigated for comparison. Figure 2 gives the sorption results of PBI and P84 dense films in water and acetone after 1 week and 1 month, respectively. After 1-week immersion, the P84 membrane shows a degree of swelling in acetone almost 12 times higher than that of water (0.14 g acetone/g membrane vs. 0.011 g water/g membrane), whereas PBI shows a much higher water uptake than acetone uptake (0.064g water/g membrane vs. 0.028 g acetone/g membrane). This is probably due to the fact that PBI is highly hydrophilic,[27] so that it takes up much more water at a faster rate than P84, whereas P84 material may be more easily attacked by acetone.

However, this situation changes after 1-month immersion, the neat PBI film shows a higher acetone uptake than water, reversing the sorption selectivity towards acetone. The sorption selectivity toward acetone may be attributed to strong hydrogen bonding interactions between the carbonyl group of acetone and the amine functional group of PBI. The

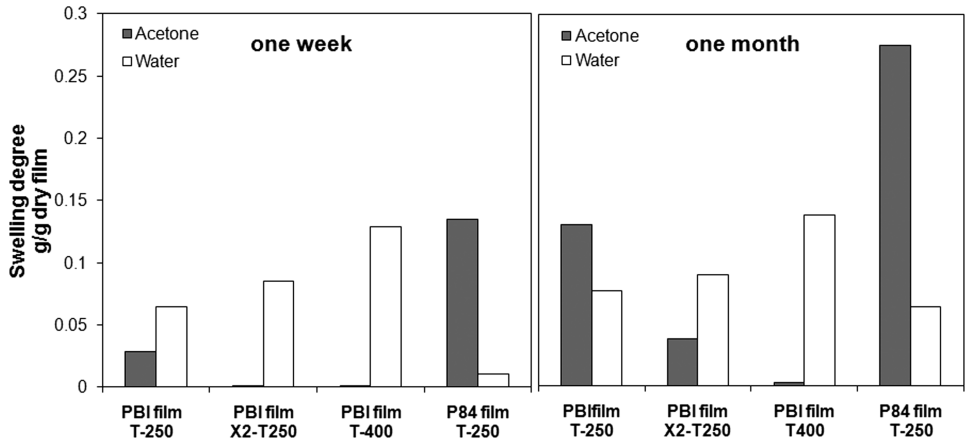

Figure 2. Sorption results of PBI and P84 dense films after one-week and one-month immersion in acetone and water.

sorption results show that PBI has higher affinity to water and lower swelling by acetone than those of P84. This is due to the fact that PBI has a closer solubility parameter to water than P84; whereas P84 has a closer solubility parameter to acetone than PBI (as shown in Table 1).

Membrane morphology of the PBI/P84 dual-layer hollow fiber membrane

Figure 3 displays the morphology of an as-spun PBI/P84 dual-layer fiber studied by FESEM. The hollow fiber has a diameter of about 653 μm. The overall wall thickness is about 114 μm and the outer layer thickness is about 30 μm. The outer edge of the outer layer reveals a dense structure at a high magnification ($\times$50,000), which is a defect-less selective layer, while the inner surface of the inner layer is very porous, which is desirable because it does not constitute much transport resistance. There is no delamination observed at the interface of the inner- and outer-layer, indicating a good adhesion.

A seamless interface may be obtained depending on the miscibility of inner layer and outer layer dopes and many other factors during phase inversion.[41] The formation of the desired interface between P84 and PBI layers in this study can be attributed to three factors. (1) Good compatibility of PBI and P84 materials. It has been extensively reported that PBI is miscible with most polyimides at a molecular level.[17,42,43] A dense film cast from a PBI/P84 blend (50/50 wt/wt) show fully homogeneous and transparent, indicating a good miscibility between these two polymers. (2) Interpenetration occurs between these two dopes because of the interfacial diffusions and convections driven by chemical potential differences. (3) A common solvent (DMAc) is used in the spinning solutions of both layers that facilitates mutual diffusion.

Effect of thermal treatment on PBI/P84 dual-layer hollow fibers

The as-spun PBI/P84 dual-layer hollow fiber membrane shows an acetone/water separation factor of only 2.2 and a

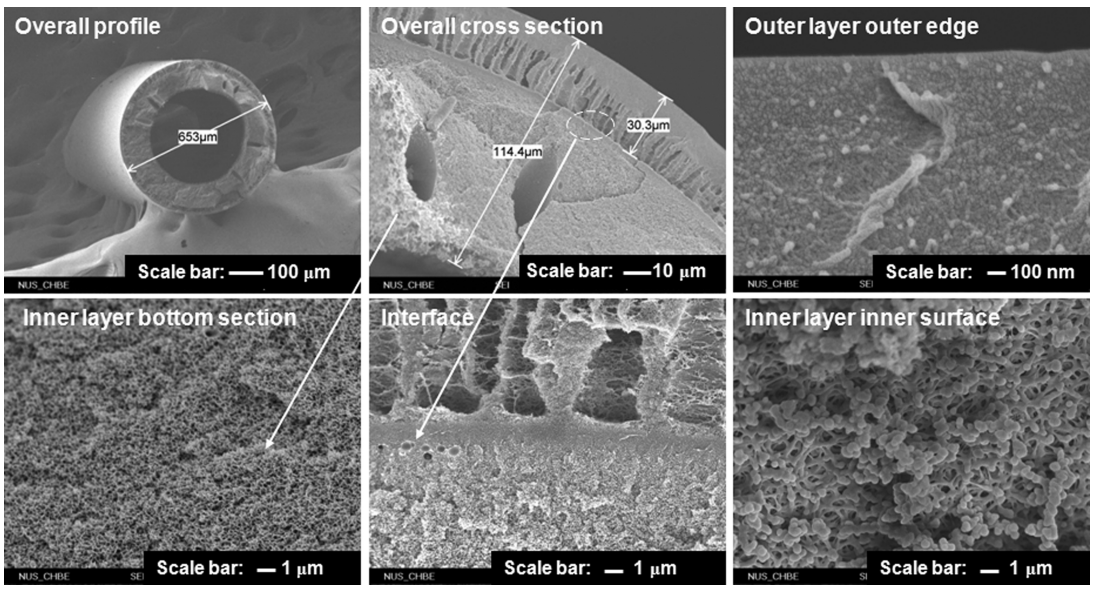

Figure 3. FE-SEM images of the cross-section morphology of the original PBI/P84 dual-layer hollow fiber.

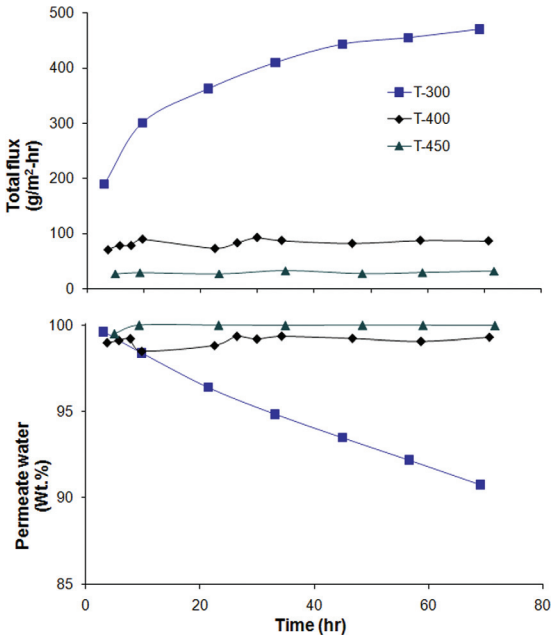

Figure 4. Pervaporation performances of PBI/P84 dual-layer hollow fibers thermal treated at different temperatures.

[Color figure can be viewed in the online issue, which is available at wileyonlinelibrary.com.]

flux of 5900 g/m^{2}h. Thus, the pervaporation test was ended after 8 h because of very low-separation factor. Figure 4 shows the pervaporation performance of dual-layer hollow fiber membranes after thermal treatments at various temperatures. As swelling by feed components on membranes especially acetone is a major concern, pervaporation tests up to 3 days are carried out to ascertain their performance stability. Based on the water purity in the permeate, a thermal treatment at 300°C improves the separation factor a lot initially (i.e., a water/acetone separation factor of 339.6). However, the impressive separation performance is not sustainable as those membranes thermal-treated at 400°C and above. Only fibers thermally treated at 400 and 450°C display sustainable separation performance. This arises from the fact that thermal treatment induces polymeric chain relaxation and packing, and crosslinking reactions. As a consequence, the thermally treated membranes have fewer defects in their thin dense-selective layers with enhanced separation factors but reduced fluxes.[17]

It has been reported that PBI may undergo free-radical crosslinking reactions at temperatures above 450°C.[44,45] The dissolution tests in the DMAc solvent confirm this hypothesis. As shown in Figure 5, PBI dense films thermally treated at 250 and 300°C can dissolve in DMAc completely within a few hours, whereas PBI films thermally treated at 400 and 450°C can only dissolve partially even after 1-month immersion in DMAc.

The variation of XRD patterns with thermal treatment (Figure 6) suggests that there may exist the occurrence of chain rearrangement in membranes even though the XRD peak apparently does not shift much with increasing thermal treatment temperature. The disappearance of smaller *d*-space of the original fiber on thermal treatment is not fully understood and will be studied in the future. Figure 7 shows the SEM morphology of dual-layer hollow fibers as a function of thermal treatment temperature and illustrates that thermal treatment at 400°C or higher leads to significant densification in the top skin layer.

To demonstrate the superiority of dual-layer over single-layer configuration, pervaporation dehydration of acetone was also conducted using both PBI single-layer and P84 single-layer hollow fiber membranes with the same thermal treatment at 400°C for a comparison. As listed in Table 4, the results reveal that neither PBI nor P84 single-layer hollow fiber membranes alone has the comparable pervaporation performance as that of PBI/P84 dual-layer hollow fiber membranes. As PBI is much hydrophilic, the water-induced swelling may increase the substructure resistance and reduce the overall separation performance of PBI single-layer hollow fiber membrane. The use of P84 as the supporting layer material can help minimize the swelling problem in the substructure and maximize the separation performance of the PBI selective layer. As a result, the synergistic effect of combining these two materials' strengths come true by means of dual-layer hollow fiber configuration.

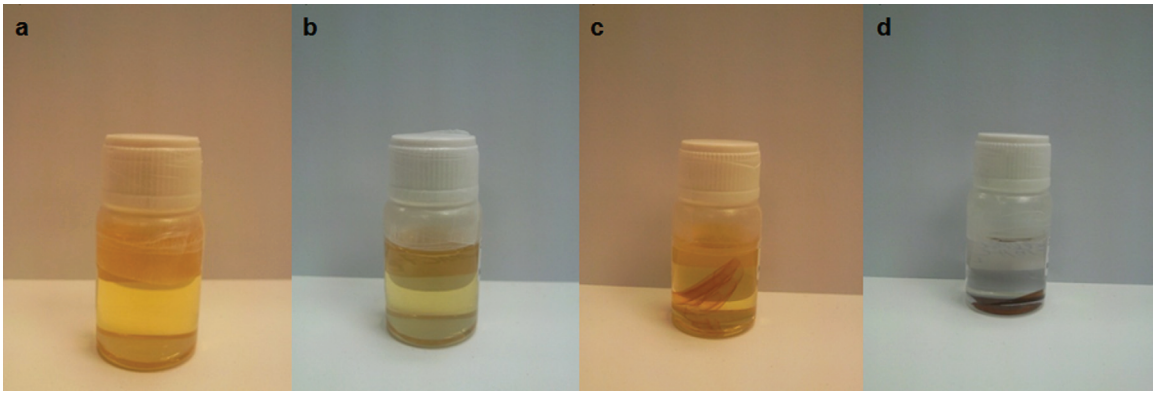

Figure 5. Dissolution results of PBI dense films in DMAc after one-month immersion.

(**a**) T-250 (fully dissolved), (**b**) T-300 (fully dissolved), (**c**) T-400, and (**d**) T-450. [Color figure can be viewed in the online issue, which is available at wileyonlinelibrary.com.]

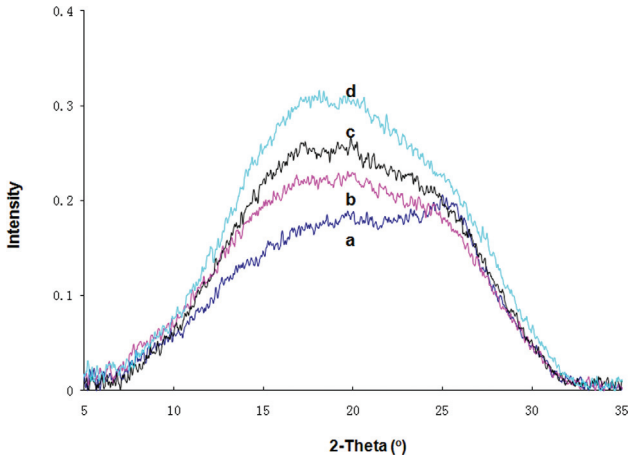

Figure 6. XRD results of (a) original PBI/P84 dual-layer hollow fiber and PBI/P84 dual-layer hollow fibers thermally treated at (b) 250°C (T-250), (c) 300°C (T-300), and (d) 400°C (T-400).

[Color figure can be viewed in the online issue, which is available at wileyonlinelibrary.com.]

Thermal treatment of chemical crosslinked PBI/P84 dual-layer hollow fibers

Chemical crosslinking has been an important means to solve the membrane swelling problem. PBI fibers were modified with *p*-xylene dichloride and undergo a reaction, which involves crosslinking between the N—H functional group of PBI molecules and the chlorine functional group of *p*-xylene dichloride[28] as illustrated in Figure 8. Figure 9 shows the FTIR spectra of PBI/P84 fibers cross-linked with 2 wt % of *p*-xylene dichloride followed by thermal treatment at various temperatures for 2 h. The formation of 1-methylimidazole group (indicated with dotted circle in Figure 8) is reflected by the appearance of the characteristic C—N peak at 1062 cm^{-1}, and the diminishment of N—H band vibration at 1293 cm^{-1}.[46] The intensity of band 1062 cm^{-1} of the thermal-treated fibers is significantly higher than those of the original fiber and the crosslinked fiber without thermal treatment. The IR peak of non-hydrogen bonded N—H at 3417 cm^{-1} reduces as thermal treatment temperature increases.[28] Thermal treatment after crosslinking may facilitate the crosslinking reaction by removing the byproduct hydrogen chloride, therefore, help to stabilize the membrane structure.[29]

Figure 10 presents the pervaporation performance of PBI/P84 fibers as a function of crosslinking conditions without additional post thermal treatment. An increase in crosslinking solution's concentration or duration time improves separation factor to some degrees but reduces flux. In addition, the performance enhancement levels off quickly if the solution concentration is further increased or deteriorates if the reaction duration is further prolonged. These unsatisfactory phenomena may be due to the fact that the crosslinking reaction is not complete and the crosslinking solvent also induces another swelling.

To uncover an effective post-treatment protocol, the sequence of modifications (i.e., thermal treatments and then crosslinking modification, or vise versa) is studied. Fibers crosslinked by 2 wt % solution concentration and 2-h duration are selected. The results listed in Table 5 show that separation factors in both sequences increase while fluxes decrease. However, the PBI/P84 fiber thermally treated at 250°C and then crosslinked achieves a much lower separation factor, when compared with the fiber crosslinked and then thermally treated at 250°C. This demonstrates that the post-thermal treatment of crosslinked hollow fibers not only

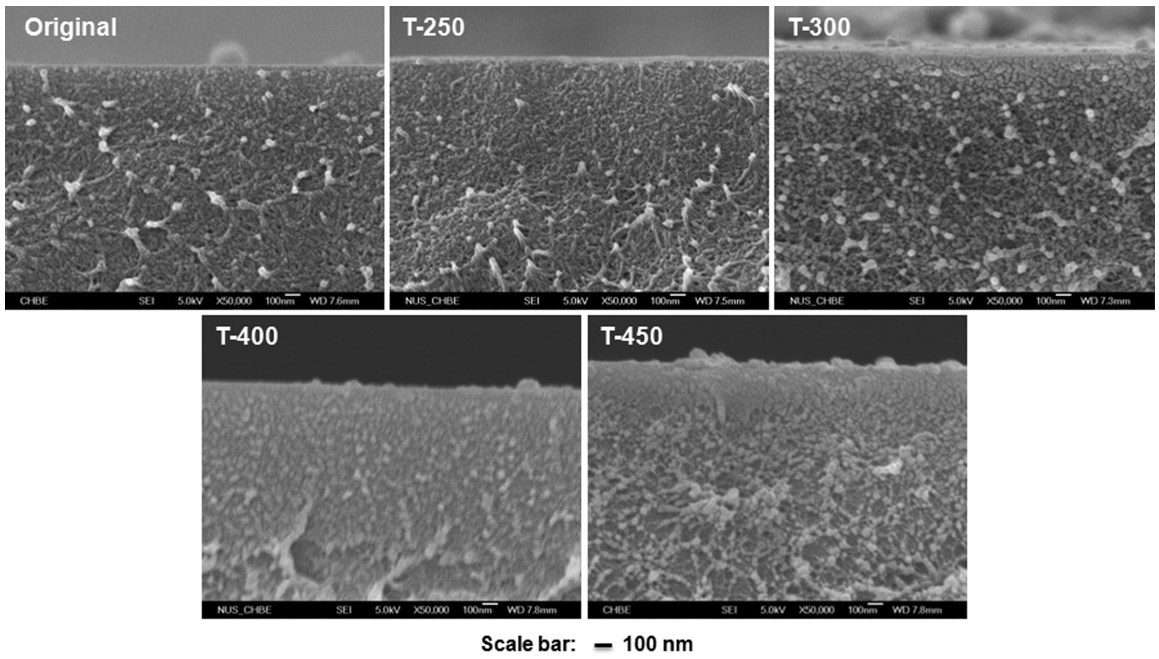

Figure 7. FE-SEM images of the cross-section morphology of the outer layer outer edge of original and thermal-treated PBI/P84 dual-layer hollow fibers at various temperatures.

Table 4. A Comparison on Separation Performances of PBI, P84 Single-Layer Hollow Fibers and PBI/P84 Dual-Layer Hollow Fiber with the Same Thermal Treatment at 400°C for 2 h

Fiber	Flux (g/m^2h)	Separation Factor (Water/Acetone)
PBI single layer	65	107
P84 single layer	183	87
PBI/P84 dual layer	80	686

help complete the crosslinking reaction but also minimize methanol-induced swelling. Thus, a synergism effect on separation performance is obtained. On the other hand, if the thermal treatment is conducted before the crosslinking modification, the thermally treated hollow fiber will have a much densified structure, which retards the diffusion of crosslinking agent into the dense-selective layer. As a result, the degree of crosslinking is reduced, and the membrane structure is not stabilized as discussed in first paragraph of the section.

Figure 12 displays the SEM morphology of the top selective layer of the crosslinked PBI fibers before and after thermal treatment. Compared with those of crosslinked fibers with thermal treatment, a relative loose structure is observed on the top selective layer of nonthermally treated fiber X2. In addition, an increase in thermal treatment temperature results in a much densified selective layer in the crosslinked PBI fibers. Figure 2 also shows the sorption data of chemically crosslinked and then thermally treated PBI dense films (T-400 and X2-T250) and compare them with thermally treated PBI dense films at 250°C. Different from thermally treated films at 250°C, the chemically crosslinked and then thermally treated PBI films have a lower acetone uptake than water uptake. Clearly, the thermal treatment facilitates the completeness of crosslinking modification, not only strengthens the polymer network but also restricts acetone diffusion into membranes. As a result, the crosslinked membranes are less susceptible to acetone-induced swelling.

Figure 10 shows the effects of post-thermal treatment temperature on pervaporation performance of crosslinked PBI/P84 hollow fibers for acetone dehydration. Both X2-T250 and X2-T300 fibers show stable separation performance for 3-day tests, while separation performance of fiber X2-T150 declines drastically even within the first day. The unstable separation performance is due to the acetone-induced swelling on fiber X2-T150, because the post-thermal treatment temperature is not high enough to stabilize the structure. Therefore, to suppress the acetone-induced swelling over time, it is essential to crosslink and then thermally treat the membrane at elevated temperatures. Compared with hollow fibers thermally treated at 400°C or above but without chemical crosslinking as shown in Figure 4, the hollow fibers chemically crosslinked and then thermally treated at low temperatures (250 or 300°C) can achieve higher fluxes and similar separation factors as illustrated in Figure 11. For example, the fiber T400 has a flux of 80 g/m^2-h and a separation factor of 686 at 50°C for a feed containing 85 wt % acetone; while the crosslinked and thermally treated fiber at 300°C has a flux of 114 g/m^2-h and a separation factor of 593. Clearly, the combination of chemical crosslinking modification and thermal treatment result in synergistic separation performance for PBI/P84 hollow fibers.

The effect of feed temperature on membrane performance

The separation performance of a pervaporation membrane is a combined result of the membrane intrinsic properties and the external operating conditions (such as feed concentration, operational temperature, downstream vacuum and other factors). At the same time, changing the operating conditions may also cause the changes of membrane structure and the mutual interactions with feed components, which consequently contribute to the alteration of mass transport coefficient of each component.[17,32–38,47] In this section, the effect of operational temperature on pervaporation performance of PBI/P84 hollow fibers membranes is investigated.

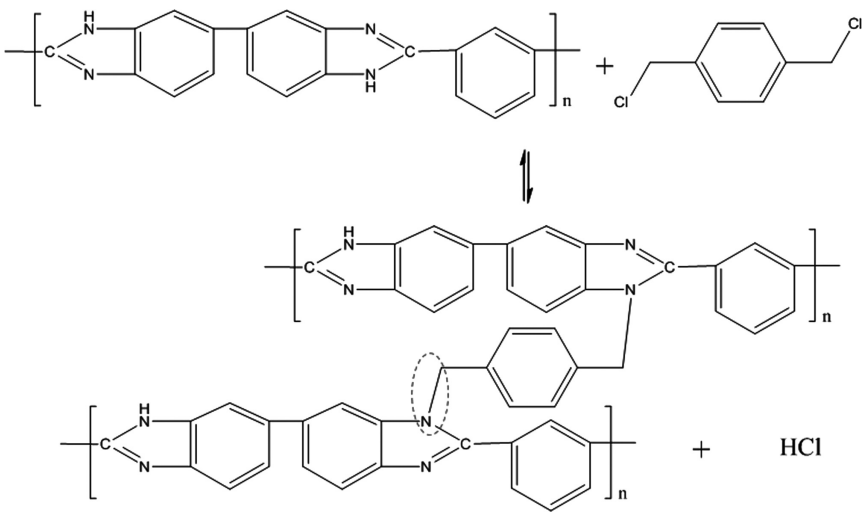

Figure 8. Proposed mechanism for the chemical crosslinking modification of PBI using *p*-xylene dichloride.

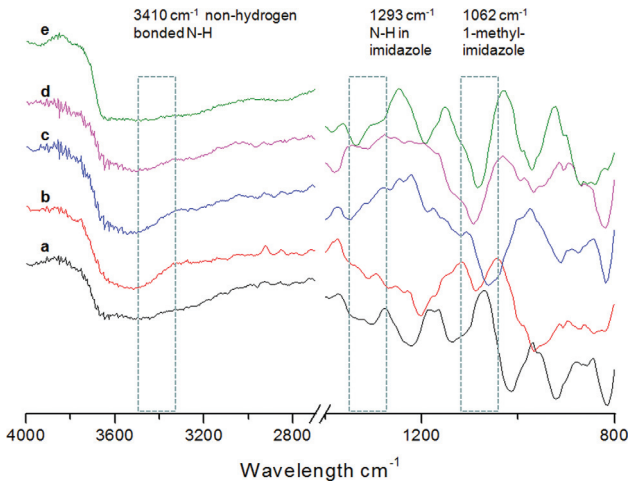

Figure 9. ATR-FTIR spectra of original and crosslinked PBI/P84 dual-layer hollow fibers followed by various thermal treatment.

(**a**) Original, (**b**) X2, (c) X2-T150, (**d**) X2-T250, and (**e**) X2-T300. [Color figure can be viewed in the online issue, which is available at wileyonlinelibrary.com.]

Fibers X2-T300 and T-400 are chosen for this study due to their relative stable separation performance.

Figure 13 shows the results and indicates that the operational temperature plays a significant role on pervaporation performance. In most conventional cases, permeation flux increases while separation factor declines with an increase in operating temperature. Interestingly, we observe an up-and-down trend of separation factor and an increased flux with an increase in feed temperature from 50 to 70°C. The enhanced separation factor and flux can be attributed to the increase of permeants vapor pressures at the feed side and the increased interstitial space between polymeric chains as a function of temperature. To exclude the external operating conditions and investigate the intrinsic properties of the membrane under different operational temperature, we convert the flux and separation factor to permeance and selectivity according to the Eq. (4).

As shown in Figure 13, the total permeance of fiber X2-T300 levels off, whereas the total permeance of fiber T-400 continuously increases when the feed temperature exceeds 60°C. The water/acetone selectivity of fibers X2-T300 and T-400 still show an up-and-down trend with an increase in feed temperature. The up-and down phenomenon may be explainable from many factors. In addition to having a lower viscosity, acetone has a much lower boiling point than water (56.53°C vs. 100°C), thus acetone may be partially in the vapor state, while water in the liquid state across the membrane when the operation temperature is greater than 60°C, and the downstream is under vacuum. Figure 14 shows that they have quite different vapor pressures. Although the partial vapor pressure of water is much lower than that of acetone, their ratio increases with an increase in feed temperature. As a result, the water/acetone selectivity increases initially with increasing feed temperature. However, a further increase in feed temperature may enlarge the interstitial space between polymeric chains, which contributes greatly to acetone vapor diffusivity and thus causes the selectivity to decline.

Generally, the temperature dependency of pervaporation flux can be described by the Arrhenius equation[48]:

$$J = J_o \exp(-E_J/\mathrm{RT}) \tag{5}$$

where J_0 are the pre-exponential factors, T is the operating temperature. E_J, the apparent activation energies of flux, can be calculated from the plot of flux vs. operational temperature using the least square method and Figure 15 presents their Arrhenius plots. The calculated activation energies of water permeation flux to cross the fibers X2-T300 and T-400 are 53.0 and 60.0 kJ/mol, respectively. The energy barrier of water transport through fiber T-400 is greater than that of fiber X2-T300. These values are consistent with our previous hypothesis that water transport across the thermally treated fiber T-400 (thermally treated at 400°C) requires a higher energy due to the much densified selective layer than the fiber X2-T300 (chemically crosslinked and thermally treated at 300°C).

PALS characterization on PBI/P84 fibers

Positron-electron annihilation γ-rays are related to electronic and free volume properties of the studied materials.[49,50] S-parameter of DBES, an indicator of free volume content, was obtained at different positron incident energy. The positron incident energy, E (KeV), is correlated to the

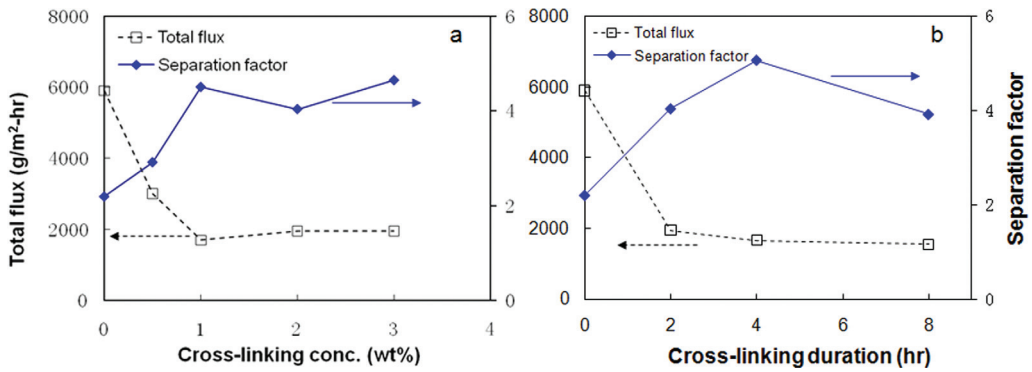

Figure 10. Pervaporation performances of crosslinked PBI/P84 dual-layer hollow fibers with (a) different crosslinking concentrations and (b) different crosslinking durations with 2 wt % *p*-xylene dichloride/methanol.

[Color figure can be viewed in the online issue, which is available at wileyonlinelibrary.com.]

Table 5. The Sequence Effect of Thermal Treatment and Crosslinking Modification on Separation Performances of PBI/P84 Dual-Layer Hollow Fibers

Post-treatment	Flux (g/m^{2}h)	Separation Factor (Water/Acetone)
Thermal treatment at 250°C	1243	7.19
Thermal treatment at 250°C followed by crosslinking modification	923	15.0
Crosslinking modification followed by thermal treatment at 250°C	300	498

mean depth Z (nm) of the polymeric material according to following equation.[39]

$$Z = \frac{40}{\rho} E^{1.6} \tag{6}$$

where ρ is the density of the polymer material in g/cm^3. Figure 16 shows all S-parameters of tested fibers. The S-parameter increases with increasing membrane depth and reaches a plateau at about 1 μm depth, suggesting that the relative free volume of membrane is the highest at this mean depth. Through the comparison of the original fiber and fibers T-250, T300, and T400, a decreasing trend of S-parameter with thermal-treatment temperature is observed, implying the reduction of free volume content, which correlates well with a flux reduction of thermally treated fibers. Compared with other crosslinked fibers, a more obvious reduction of S-parameter in the X2 fiber suggests that thermal treatment after crosslinking reduces the relative free volume. A relatively higher free volume of the X2 fiber may be caused by the methanol-induced swelling during the crosslinking modification.

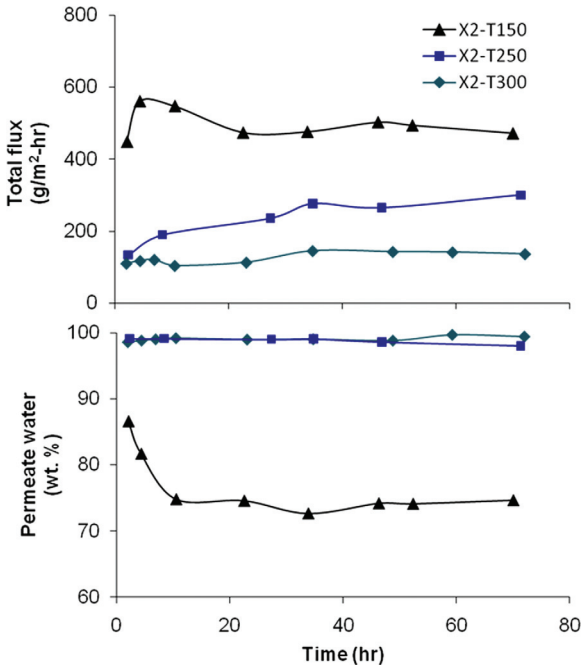

Figure 11. Pervaporation performances of crosslinked PBI/P84 dual-layer hollow fibers followed by thermal treatment at different temperatures.

[Color figure can be viewed in the online issue, which is available at wileyonlinelibrary.com.]

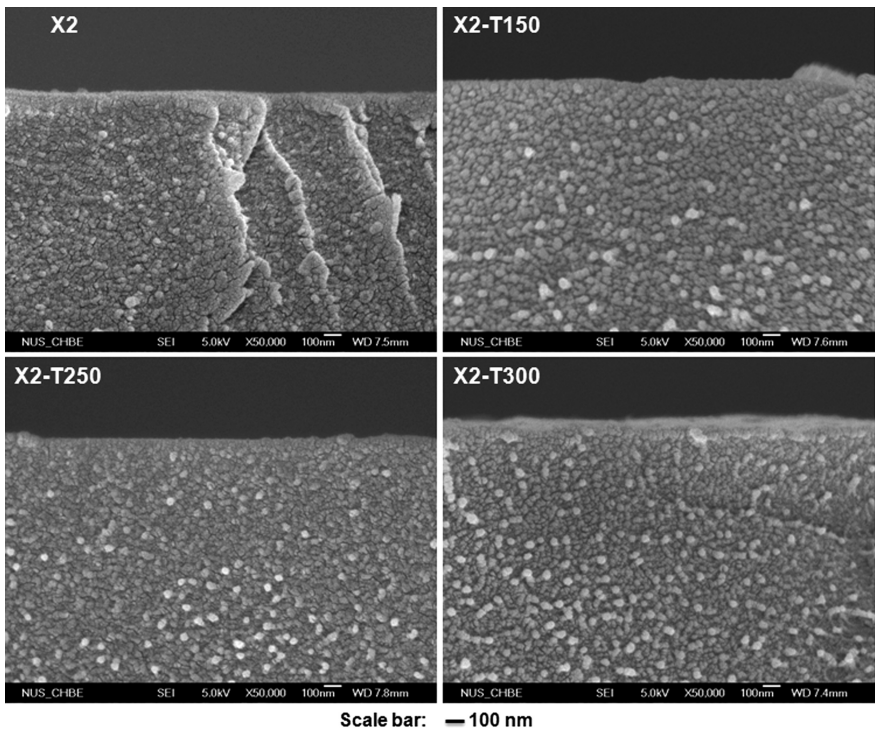

Figure 12. Cross-section morphology of the outer layer outer edges of crosslinked PBI/P84 dual-layer hollow fibers thermally treated at various temperatures.

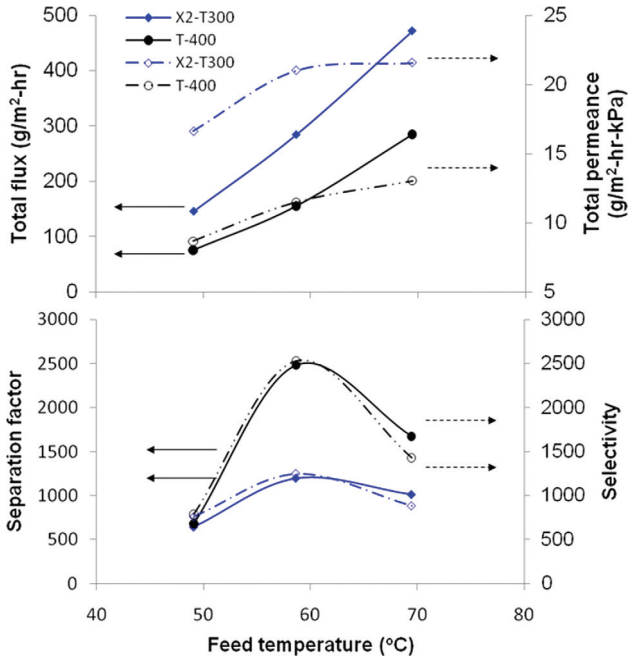

Figure 13. Feed temperature effect on pervaporation performances of modified PBI/P84 dual-layer hollow fibers (Solid line: total flux and separation factor; dashed line: total permeance and selectivity).

[Color figure can be viewed in the online issue, which is available at wileyonlinelibrary.com.]

Quantitative calculations of the free volume at a scale of 0.2–2 nm can be carried out using the PATFIT[40] program and Tao model[51] with the aid of O-Ps lifetime (t_3) and intensity (I_3) values measured from PALS on the dense selective layer. The relative fractional free volume (FFV) is determined according to the following equation.[52]

$$\mathrm{FFV}(\%) = 0.0018 I_3 f_v \tag{7}$$

where $f_v = (4/3)\pi R^3$ is the average of the o-Ps hole size and R is the free volume radius. The FFV value determined from pick-off o-Ps annihilation is different from the traditional

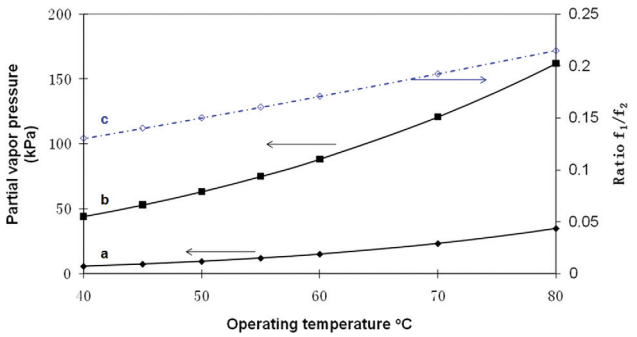

Figure 14. Partial vapor pressures of (a) water; (b) acetone; and (c) the vapor pressure ratio of water/acetone at the feed side.

[Color figure can be viewed in the online issue, which is available at wileyonlinelibrary.com.]

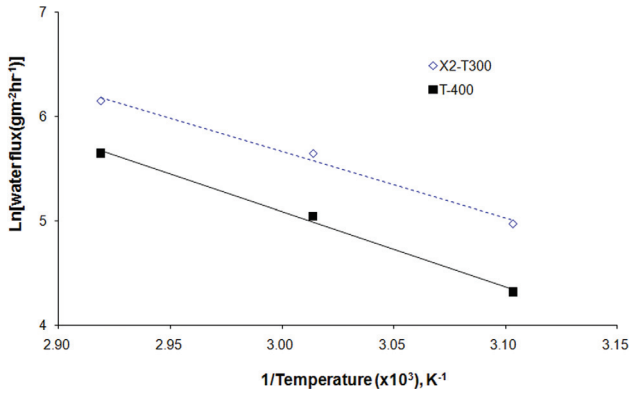

Figure 15. The Arrhenius plots of PBI/P84 dual-layer hollow fibers X2-T300 and T-400.

[Color figure can be viewed in the online issue, which is available at wileyonlinelibrary.com.]

Bondi's method,[39,53] the former usually has a smaller FFV value than the latter. Table 6 summarizes the lifetime data of the original fibers and modified fibers T-400 and X2-T300 measured by 1 keV positron incident energy that is equivalent to 30.5-nm depth from the membrane surface. This depth is believed to be within the dense selective layer. The fractional free volume of the PBI selective layer reduces from 3.27 to 1.98% (T-400) and 1.33% (X2-T300), respectively, after thermal treatment and a combination of chemical/thermal crosslinking modifications. These values correlate well with pervaporation data where significant flux drops have been observed for post-treated fibers. In summary, both chemical crosslinking reactions and thermally induced modifications are effective to lower membrane free volume and increase diffusivity selectivity, while a combination of chemical/thermal crosslinking modifications appears to be superior.

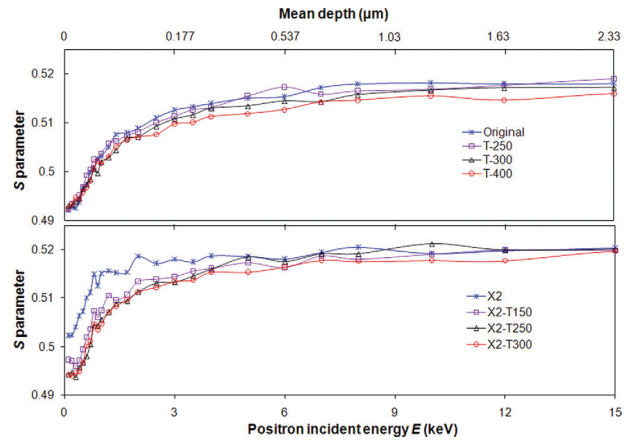

Figure 16. *S* parameter vs. positron incident energy (or membrane depth) of the outer layer of PBI/P84 dual-layer hollow fibers outer layer with (A) different thermal treatments and (B) crosslinking modification followed by different thermal treatments.

[Color figure can be viewed in the online issue, which is available at wileyonlinelibrary.com.]

Table 6. O-Ps Lifetime Results of PBI/P84 Dual-Layer Hollow Fibers at 1 keV Positron Incident Energy

PBI/P84 fiber	τ_3 (ns)	I3 (%)	R (Å)	fv (Å^3)	ffv (%)
Original	2.01 ± 0.04	18.4 ± 0.56	2.86 ± 0.03	98.3 ± 3.36	3.27 ± 0.21
T-400	1.83 ± 0.04	13.4 ± 0.39	2.70 ± 0.03	82.3 ± 2.78	1.98 ± 0.12
X2-T300	1.70 ± 0.05	10.5 ± 0.51	2.56 ± 0.04	70.4 ± 3.62	1.33 ± 0.13

fv (free volume) = $4\pi R^3/3$
ffv % (relative fractional free volume %) = $0.0018 I_3 f_v$[52].

Conclusions

We have fabricated PBI/P84 dual-layer hollow fiber membranes by the coextrusion phase inversion for acetone dehydration. The dual-layer hollow fiber has a seamless interface, a selective PBI outer layer, and a porous P84 inner layer, which is very desirable for pervaporation. The effects of heat treatment and chemical crosslinking modifications on membranes morphology, pervaporation performance, and fractional free volume have been investigated. The following conclusions can be drawn:

i) Swelling results reveal that PBI has a higher affinity to water and a lower swelling by acetone than those of P84.

ii) Thermal treatment of PBI/P84 dual-layer fibers at 400°C and higher improves separation factor but reduces flux severely because of excessive densification.

iii) PBI/P84 fibers thermally treated at 300°C show impressive but unstable separation performance because of high degrees of acetone-induced swelling.

iv) Crosslinking by *p*-xylene dichloride followed by a thermal treatment above 250°C show effectiveness to stabilize membrane structure and significantly improve separation performance.

v) Although the stability of PBI/P84 fibers against acetone can be achieved through thermal-induced crosslinking reactions at high temperatures, chemically crosslinked PBI/P84 fibers show better fluxes due to thinner dense selective layers.

vi) An optimum feed temperature of 60°C is found for the pervaporation dehydration of acetone. The resultant performance of the X2-T300 PBI/P84 membrane has a permeation flux of 0.284 kg/m^2-h and a separation factor of 1187 for a feed containing 85 wt % acetone.

vii) The selective layer thickness and relative FFV have been determined by PALS. The relative FFV of the PBI selective layer reduces from 3.27% for the original fiber to 1.98 and 1.33% for T-400 and X2-T300 fibers, respectively.

Acknowledgments

The authors thank A-STAR and NUS (R-279-000-288-305) for funding this research. Special thanks are due to Dr. Natalia Widjojo, Dr. Youchang Xiao, Dr. Jincai Su, Dr. Na Peng, Dr. Kaiyu Wang, Mr. Fuyun Li, Miss Mei Ling Chua, Miss Huan Wang and Miss Sui Zhang for their valuable discussions and help. The authors also thank Mr. Yee Kang Ong for the sorption data of P84 membrane.

Literature Cited

1. Green MM, Wittcoff HA. *Organic Chemistry Principles and Industrial Practice*. Wiley-VCH, Weinheim. 2003.
2. Sifniades S, Levy AB. Acetone. Ullmann's Encyclopedia of Industrial Chemistry. Wiley-VCH, Weinheim. 2005.
3. Banat FA, Al-Rub FAA, Simandl J. Isothermal vapor-liquid equilibrium of acetone-water mixture in the presence of molecular sieves. *Sep Sci Technol*. 2001;36:487–497.
4. Lue SJ, Ou JS, Kuo CH, Chen HY, Yang TH. Pervaporative separation of azeotropic methanol/toluene mixtures in polyurethane-poly (dimethylsiloxane) (PU-PDMS) blend membranes: correlation with sorption and diffusion behaviors in a binary solution system. *J Membr Sci*. 2010;347:108–115.
5. Tsai HA, Chen WH, Kuo CY, Lee KR, Lai JY. Study on the pervaporation performance and long-term stability of aqueous iso-propanol solution through chitosan/polyacrylonitrile hollow fiber membrane. *J Membr Sci*. 2008;309:146–155.
6. Huang Y, Vane LM. BioSep^{TM}: A New Ethanol Recovery Technology for Small Scale Rural Production of Ethanol from Biomass. American Institute of Chemical Engineers 2006 Annual Meeting, San Francisco, CA.
7. Vane LM, Namboodiri VV, Bowen TC. Hydrophobic zeolite–silicone rubber mixed matrix membranes for ethanol–water separation: effect of zeolite and silicone component selection on pervaporation performance. *J Membr Sci*. 2008;308:230–241.
8. Jiang LY, Wang Y, Chung TS, Qiao XY, Lai JY. Polyimides membranes for pervaporation and biofuels separation. *Prog Polym Sci*. 2009;34:1135–1160.
9. Bowen TC, Noble RD, Falconer JL. Fundamentals and applications of pervaporation through zeolite membranes. *J Membr Sci*. 2004;245:1–33.
10. Wang KY, Chung TS, Rajagopalan R. Dehydration of tetrafluoropropanol (TFP) by pervaporation via novel PBI/BTDA-TDI/MDI copolyimide (P84) dual-layer hollow fiber membranes. *J Membr Sci*. 2007;287:60–66.
11. Qiao XY, Chung TS. Fundamental characteristics of sorption, swelling, and permeation of P84 co-polyimide membranes for pervaporation dehydration of alcohols. *Ind Eng Chem Res*. 2005;44:8938–8943.
12. Hosseini SS, Teoh MM, Chung TS. Hydrogen separation and purification in membranes of miscible polymer blends with interpenetration networks. *Polymer*. 2008;49:1594–1603.
13. Peng F, Lu L, Sun H, Jiang Z. Analysis of annealing effect on pervaporation properties of PVA-GPTMS hybrid membranes through PALS. *J Membr Sci*. 2006;281:600–608.
14. Huang RYM, Pal R, Moon GY. Crosslinked chitosan composite membrane for the pervaporation dehydration of alcohol mixtures and enhancement of structural stability of chitosan/polysulfone composite membranes. *J Membr Sci*. 1999;160:17–30.
15. Yang JM, Su WY, Leu TL, Yang MC. Evaluation of chitosan/PVA blended hydrogel membranes. *J Membr Sci*. 2004;236:39–51.
16. Inui K, Okumura H, Miyata T, Uragami T. Permeation and separation of benezene/cycloxane mixtures through cross-linked poly(alkyl methacrylate) membranes. *J Membr Sci*. 1997;132:193–202.
17. Chung TS, Guo WF, Liu Y. Enhanced Matrimid membranes for pervaporation by homogenous blends with polybenzimidazole (PBI). *J Membr Sci*. 2006;271:221–231.
18. Chen JH, Liu QL, Zhu AM, Zhang QG. Dehydration of acetic acid by pervaporation using SPEK-C/PVA blend membranes. *J Membr Sci*. 2008;320:416–422.
19. Wang XP, Li N, Wang WZ. Pervaporation properties of novel alginate composite membranes for dehydration of organic solvents. *J Membr Sci*. 2001;193:85–95.
20. Zhang W, Li G, Fang Y, Wang X. Maleic anhydride surface-modification of crosslinked chitosan membrane and its pervaporation performance. *J Membr Sci*. 2007;295:130–138.

21. Burshe MC, Netke SA, Sawant SB, Joshi JB, Pangarkar VG. Pervaporative dehydration of organic solvents. *Sep Sci Technol*. 1997;32:1335–1349.
22. Ray S, Ray SK. Effect of copolymer type and composition on separation characteristics of pervaporation membranes—a case study with separation of acetone–water mixtures. *J Membr Sci*. 2006;270:73–87.
23. Ray S, Ray SK. Dehydration of acetic acid, alcohols, and acetone by pervaporation using acrylonitrile-maleic anhydride copolymer membrane. *Sep Sci Technol*. 2005;40:1583–1596.
24. Zhao Q, Qian J, An Q, Zhu Z, Zhang P, Bai Y. Studies on pervaporation characteristics of polyacrylonitrile–b-poly(ethylene glycol)–b-polyacrylonitrile block copolymer membrane for dehydration of aqueous acetone solutions. *J Membr Sci*. 2008;311:284–293.
25. Amnuaypanich S, Ratpolsan P. Pervaporation membranes from natural rubber latex grafted with poly(2-hydroxyethyl methacrylate) (NR-g-PHEMA) for the separation of water–acetone mixtures. *J Appl Polym Sci*. 2009;113:3313–3321.
26. Urtiaga AM, Casado C, Aragoza C, Ortiz I. Dehydration of industrial ketonic effluents by pervaporation. Comparative behavior of ceramic and polymeric membranes. *Sep Sci Technol*. 2003;38:3473–3491.
27. Chung TS. A critical review of polybenzimidazoles: historical development and future R & D. *Rev Macromol Chem Phys C*. 1997;37:277–301.
28. Wang KY, Xiao YC, Chung TS. Chemically modified polybenzimidazole nanofiltration membrane for the separation of electrolytes and cephalexin. *Chem Eng Sci*. 2006;61:5807–5817.
29. Jorgensen BS, Young JS, Espinoza BF. Cross-linked polybenzimidazole membrane for gas separation. US Patent 6,946,015.
30. Li Q, Jensen JO, Savinell RF, Bjerrum NJ. High temperature proton exchange membranes based on polybenzimidazoles for fuel cells. *Prog Polym Sci*. 2009;34:449–477.
31. Wang Y, Chung TS. Pervaporation dehydration of ethylene glycol through polybenzimidazole (PBI)-based membranes. 1. Membrane fabrication. *J Membr Sci*. 2010;363:149–159.
32. Liu RX, Qiao XY, Chung TS. Dual-layer P84/polyethersulfone hollow fibers for pervaporation dehydration of isopropanol. *J Membr Sci*. 2007;294:103–114.
33. Jiang LY, Chen H, Jean YC, Chung TS. Ultrathin polymeric interpenetration network with separation performance approaching ceramic membranes for biofuel. *AIChE J*. 2009;55:75–86.
34. Wang Y, Goh SH, Chung TS, Peng N. Polyamide-imide/polyetherimide dual-layer hollow fiber membranes for pervaporation dehydration of C1-C4 alcohols. *J Membr Sci*. 2009;326:222–233.
35. Widjojo N, Chung TS. Pervaporation dehydration of C2-C4 alcohols by 6FDA-ODA-NDA/Ultem® dual-layer hollow fiber membranes with enhanced separation performance and swelling resistance. *Chem Eng J*. 2009;155:736–743.
36. Qiao XY, Chung TS, Pramoda KP. Fabrication and characterization of BTDA-TDI/MDI (P84) co-polyimide membranes for the pervaporation dehydration of isopropanol. *J Membr Sci*. 2005;264:176–189.
37. Wang Y, Jiang LY, Matsuura T, Chung TS, Goh SH. Investigation of the fundamental differences between polyamide-imide (PAI) and polyetherimide (PEI) membranes for isopropanol dehydration via pervaporation. *J Membr Sci*. 2008;318:217–226.
38. Guo WF, Chung TS, Matsuura T, Wang R, Liu Y. Pervaporation study of water and tert-butanol mixtures. *J Appl Polym Sci*. 2004;91:4082–4090.
39. Jean YC, Mallon PE, Schrader DM. *Principles and Applications of Positron and Positronium Chemistry*. World Scientific Publishing Co Pte Ltd. Singapore. 2003.
40. Chen H, Hung WS, Lo CH, Huang SH, Cheng ML, Liu G, Lee KR, Lai JY, Sun YM, Hu CC, Suzuki R, Ohdaira T, Oshima N, Jean YC. Free-volume depth profile of polymeric membranes studied by positron annihilation spectroscopy: layer structure from interfacial polymerization. *Macromolecules*. 2007;40:7542–7557.
41. Li DF, Chung TS, Wang R. Morphological aspects and structure control of dual-layer asymmetric hollow fiber membranes formed by a simultaneous coextrusion approach. *J Membr Sci*. 2004;243:155–175.
42. Musto P, Karaszt FE, Macknight WJ. Hydrogen bonding in polybenzimidazole/ polyimide systems: a Fourier-transform infra-red investigation using low-molecular-weight monofunctional probes. *Polymer*. 1989;30:1012–1021.
43. Ahn TK, Kim M, Choe S. Hydrogen-bonding strength in the blends of polybenzimidazole with BTDA- and DSDA-based polyimides. *Macromolecules*. 1997;30:3369–3740.
44. Vogel H, Marvel CS. Polybenzimidazoles, new thermally stable polymers. *J Polym Sci*. 1961;L:511–539.
45. Gillham JK. Polymer structure: cross-linking of a polybenzimidazole. *Science*. 1963;139:494–495.
46. Noye P, Li Q, Pan C, Bjerrum JN. Cross-linked polybenzimidazole membranes for high temperature proton exchange membrane fuel cells with dichloromethyl phosphinic acid as a cross-linker. *Polym Adv Technol*. 2008;19:1270–1275.
47. Jiraratananon R, Chanachai A, Huang RYM, Uttapap D. Pervaporation dehydration of ethanol-water mixtures with chitosan/hydroxyethylcellulose (CS/HEC) composite membranes I. Effect of operating conditions. *J Membr Sci*. 2002;195:143–151.
48. Feng X, Huang RYM. Estimation of activation energy for permeation in pervaporation processes. *J Membr Sci*. 1996;118:127–131.
49. Park HB, Jung CH, Lee Y M, Hill AJ, Pas SJ, Mudie ST, Wagner EV, Freeman BD, Cookson DJ. Polymers with cavities tuned for fast selective transport of small molecules and ions. *Science*. 2007;318:254–258.
50. Chen H, Hung WS, Lo CH, Huang SH, Cheng ML, Liu G, Lee KR, Lai JY, Sun YM, Hu CC, Suzuki R, Ohdaira T, Oshima N, Jean YC. Free-volume depth profile of polymeric membranes studied by positron annihilation spectroscopy: layer structure from interfacial polymerization. *Macromolecules*. 2007;40:7542–7557.
51. Tao SJ. Positronium annihilation in molecular substrates. *Chem Phys*. 1972;56:5499–5510.
52. Jean YC, Yuan JP, Liu J, Deng Q, Yang H. Correlations between gas permeation and free-volume hole properties probed by positron annihilation spectroscopy. *J Polym Sci B: Polym Phys*. 1995;33:2365–2371.
53. Yampolskii Y, Pinnau I, Freeman BD. *Material Science of Membranes for Gas and Vapor Separation*. Wiltshire, Wiley, 2006.

Manuscript received Oct. 29, 2010, and revision received Mar. 2, 2011.